Cross-Institutional Structured Radiology Reporting for Lung Cancer Screening Using a Dynamic Template-Constrained Large Language Model

Chuang Niu¹, Parisa Kaviani³, Qing Lyu², Mannudeep K. Kalra³, Christopher T. Whitlow², Ge Wang¹

¹Department of Biomedical Engineering, School of Engineering, Center for Computational Innovations, Center for Biotechnology & Interdisciplinary Studies, Rensselaer Polytechnic Institute, 110 8th Street, Troy, 12180, NY, USA.

²Department of Radiology, Wake Forest University School of Medicine, Winston-Salem, 27103, NC, USA.

³Department of Radiology, Massachusetts General Hospital, Harvard Medical School, White 270-E, 55 Fruit Street, Boston, 02114, MA, USA.

ABSTRACT

Background

High-quality structured radiology reports are advantageous to optimize clinical workflows and patient outcomes. Current LLMs in creating structured reports face the challenges of formatting errors, content hallucinations, and privacy leakage concerns when uploaded to external servers.

Purpose

To develop an enhanced open-source LLM for creating structured and standardized LCS reports from free-text descriptions and establish its utility in nodule-level information retrieval and automatic large-scale statistical analysis.

Materials and Methods

After institutional IRB approvals, 5,442 de-identified LCS reports from two institutions were retrospectively analyzed. 500 reports were randomly selected from the two institutions evenly and then manually labeled for evaluation. Two radiologists from the two institutions developed a standardized template including 29 features for lung nodule reporting. We proposed template-constrained decoding to enhance state-of-the-art open-source LLMs, including LLAMA, Qwen, and Mistral. The LLM performance was extensively evaluated in terms of F1 score, confidence interval, McNemar test, and z-test. Based on the structured reports created from the large-scale dataset, a nodule-level retrieval system was prototyped and an automatic statistical analysis was performed. Our software, vLLM-structure, is publicly available for local deployment with enhanced LLMs.

Results

Our template-constrained decoding approach consistently enhanced the LLM performance on multi-institutional datasets, with neither formatting errors nor content hallucinations. Our method improved the best open-source LLAMA-3.1 405B by up to 10.42% (97.60% vs 87.18%; p-value < 0.01 for all 29 features), and outperformed GPT-40 by 17.19% (97.60% vs 80.41%; p-value <

0.01 for 27 out of 29 features). A novel nodule retrieval system was successfully prototyped and demonstrated on a large-scale multimodal database using our enhanced LLM technologies. The automatically derived statistical distributions were closely consistent with the prior findings in terms of nodule type, location, size, status, and Lung-RADS.

Conclusion

Our dedicated open-source LLM accurately created structured radiology reports for LCS across institutions, defining the state of the art in this domain. Its utility has been demonstrated in nodule-level information retrieval and automatic large-scale statistical analysis.

Abbreviations

LLM = Large Language Model, LCS = Lung Cancer Screening, LDCT = Low-Dose CT, GGN = Ground Glass Nodule, JSON = JavaScript Object Notation, CI = Confidence Interval

INTRODUCTION

Structured and standardized reporting in radiology has been recognized to improve quality, consistency, and actionability of radiology reports, leading to optimized clinical workflow and patient outcomes [1, 2]. Structured reports can be divided into two levels: structured layout (level-1) and structured content (level-2) [3]. Structured layout defines the report format to present findings with subheadings in a specific order, such as *lung nodules, lungs, pleura, heart, etc.*, in LCS. Structured content refers to writing contents with a set of predefined features, such as nodule type, lobe, margin, shape, size, etc., to describe lung nodules, and each feature has a set of predefined and standardized candidate values. Radiology reports contain rich information for research and clinical purposes. To effectively perform data mining, the radiology reports must be structured at level-2 to provide standardized, discrete data elements easier to search and analyze [4]. Despite its various benefits, structured reporting (particularly at level-2) has still not been widely adopted in clinical routine [5]. One of the major obstacles is that current structured reporting software demands radiologists' use of the mouse and many clicks on checkboxes and other graphical elements, distracting their attention from main tasks and reducing their productivity [6].

Recent advancement in LLMs has provided unprecedented opportunities to create structured radiology report seamlessly in the radiological workflow. For example, GPT-4 was leveraged to convert 170 free-text CT and MRI reports to structured reports at level-1 [7]. In a most recent study, GPT-3.5 and GPT-4 were prompted to create synoptic reports at level-1 from 180 original CT reports for pancreatic ductal adenocarcinoma, showing the GPT-4 performed better than GPT-3.5 and that surgeons demonstrated greater accuracy in categorizing respectability using the converted reports compared to the original ones [8]. However, there has been no study so far demonstrating the desired level-2 structured reporting with LLMs. Moreover, all these studies used the proprietary LLMs which require uploading radiology reports to the cloud server, raising privacy concerns especially for large-scale studies [9]. This concern can be addressed by deploying the latest and similarly powerful open-source Llama 3.1 with 405 billion parameters on the local server [10]. Importantly, such an LLM can be further developed and adapted to specific applications with enhanced performance.

There are two main challenges when applying an LLM for structured reporting: formatting errors and content hallucinations. JSON is used as a standard format to output the structured contents by LLM, but LLMs cannot ensure that the JSON format is always correct, leading to failed conversions. On the other hand, the well-known hallucinations of all LLMs cannot be tolerated in the healthcare applications [11]. These challenges must be overcome to establish an accurate and reliable LLM-based structured reporting. Additionally, while many initiatives were lunched to promote structured reporting, cross-institutional study on structured reporting is lacking [5].

Table 1: Structured Template for Lung Nodule Reporting

Features Candidate Set							
Number of Dictionaries	Integer numbers: 0-50, null						
Nodule ID	Integer numbers: 1-50, null						
Series ID	Integer numbers: 1-2000, null						
Image ID	Integer numbers: 1-5000, null						
Lobe	(1) right upper lobe, (2) right middle lobe, (3) right lower lobe, (4) left upper lobe, (5) lingula, (6) right lower lobe, (7) null						
Segment	(1) apical, (2) posterior, (3) anterior, (4) lateral, (5) medial, (6) superior, (7) medial basal, (8) anterior basal, (9) lateral basal, (10) posterior basal, (11) apico-posterior, (12) anteromedial basal, (13) inferior, (14) null						
Fissure	(1) right minor fissure, (2) right major fissure, (3) left major fissure, (4) right fissural, (5) left fissural, (6) fissural, (7) right perifissural, (8) left perifissural, (9) perifissural, (10) null						
Pleural	(1) subpleural, (2) pleural-based, (3) peripheral, null						
Tracheobronchial	(1) airway, (2) tracheal, (3) endotracheal, (4) endobronchial, (5) peribronchial, (6) peribronchovascular, (7) bronchocentric, (8) bronchovascular, (9) null						
Perihilar	(1) perihilar, (2) null						
Lung	(1) left, (2) right, (3) bilateral, (4) null						
Туре	(1) solid, (2) part-solid, (3) mixed attenuation, (4) cystic, (5) ground glass, (6) hazy, (7) nonsolid, (8) fluid/water, (9) fat, (10) calcified, (11) part-calcified, (12) noncalcified, (13) cavitary, (14) null						
Calcification Patterns	(1) diffuse, (2) central, (3) lamellated, (4) popcorn, (5) eccentric, (6) dense, (7) dendriform, (8) punctate, (9) linear, (10) null						
Margin	(1) spiculated, (2) smooth, (3) lobulated, (4) fuzzy, (5) irregular, (6) null						
Shape	(1) oval, (2) lentiform, (3) triangular, (4) round, (5) bilobed, (6) rectangular, (7) polygonal, (8) spherical, (9) irregular, (10) ovoid, (11) tubular, (12) branching, (13) null						
Long Axis (mm)	Float numbers: 0.00-200.00						
Short Axis (mm)	Float numbers: 0.00-200.00						
Third Axis (mm)	Float numbers: 0.00-200.00						
Average Diameter (mm)	Float numbers: 0.00-200.00						
Part-Solid Diameter (mm)	Float numbers: 0.00-200.00						
Volume (mm ³)	Float numbers: 0.00-10000.00						
Mass (mg)	Float numbers: 0.00-10000.00						
Qualitative Descriptor	(1) small, (2) tiny, (3) micronodule, (4) punctate, (5) subcentimeter, (6) large, (7) null						
Status	(1) stable, (2) increase, (3) decrease, (4) new, (5) changed, (6) baseline, (7) interval development, (8) resolved, (9) null						
Lung-RADS	(1) 0, (2) 1, (3) 2, (4) 3, (5) 4A, (6) 4B, (7) 4X, (8) null						
Comparison Date	01/01/2000-12/31/2050, null						
Overall Lung-RADS	(1) 0, (2) 1, (3) 2, (4) 3, (5) 4A, (6) 4B, (7) 4X, (8) null						
Recommend Imaging	(1) LDCT, (2) LDCT, PET/CT, (3) LDCT, Tissue sampling, (4) LDCT, PET/CT, Tissue sampling, (5) LDCT, Diagnostic CT, (6) LDCT, Diagnostic CT, PET/CT, (7) LDCT, Diagnostic CT, PET/CT, Tissue sampling, (8) Diagnostic CT, (9) Diagnostic CT with contrast, (10) Diagnostic CT, PET/CT, (11) Diagnostic CT with contrast, PET/CT, (12) Diagnostic CT, PET/CT, Tissue sampling, (13) Diagnostic CT with contrast, PET/CT, Tissue sampling, (14) PET/CT, (15) PET/CT, Tissue sampling, (16) Tissue sampling, (17) null						
Imaging Interval	(1) 1 month, (2) 1-2 months, (3) 1-3 months, (4) 2-3 months, (5) 3 months, (6) 3-6 months, (7) 4-6 months, (8) 6 months, (9) 6-12 months, (10) 12 months (11) null						
Follow-up Date	01/01/2000-12/31/2050, null						

Note.— Lung-RADS = Lung CT Screening Reporting and Data System

The purpose of this study is to develop the open-source LLMs for automatically creating level-2 structured reports from free-text contents, with a focus on lung nodule descriptions in LCS. We will define a cross-institutional template, curate cross-institutional evaluation datasets, and demonstrate the actionability of structured reports through nodule-level information retrieval and automatic statistical analysis on a large-scale dataset.

MATERIALS AND METHODS

Cross-Institutional Template and Evaluation Datasets

After the IRB approvals, the deidentified LDCT LCS radiology reports with the associated age and sex information were collected from a tertiary (institution-1) and a quaternary (institution-2) hospital in this retrospective and cross-institutional study. For LDCT LCS, both institutions used the level-1 structured reporting but in different formats with different groups of subheadings. Specifically, the reports in the first institution usually includes *lung nodules, COPD, severity, pleura, heart, coronary artery calcification, mediastinum/hilum/axilla, and other findings* to present findings, while the second institution usually uses *lines/tubes, lungs and airways, pleura, soft tissues, abdomen, and bones* to represent findings. In practice, different subheadings were used within the same institution. Following each subheading, various styles of free-text descriptions were written by radiologists.

Table 2: Distributions of Multi-Institutional Datasets by Age and Sex

Age	<55 y		55-65 y		65-75 y		≥75 y	
Sex	Male	Female	Male	Female	Male	Female	Male	Female
Insitution-1-Labeled	4	3	58	56	64	47	9	9
Institution-2-Labeled	7	6	62	64	50	44	8	9
Insitution-1	37	72	1122	1162	1185	1200	205	209

Note.— Institution-1-Labeled and Institution-2-Labeled mean the datasets from the first and the second institutions respectively. Each of the datasets contains 250 pairs of original and labeled structured reports. Institution-1 is the dataset including 5,192 original reports from the first institution from January 1, 2021 to December 31, 2023.

To study the feasibility of automatically creating the level-2 structured reports from the free-text reports with LLM, a standardized template was established in Table 1 by the radiologists from the two institutions. Note that this template is for research purpose with a focus on lung nodule reporting. It consists of 30 features, including 25 nodule-level features that are grouped together as a nodule descriptor to describe an individual nodule, 4 features to present patient management at report-level, and 1 feature to determine the number of nodule descriptors to be created to cover all individual lung nodules in the report. Each feature has a set of standardized terms as its candidate values. A single nodule descriptor may present multiple nodules; e.g., when the number of descriptors cannot be exactly determined from the description, such as "Small bilateral calcified nodules", then a single descriptor is created to represent these nodules. To quantitatively evaluate the performance of LLMs, 500 reports were collected and manually labeled according to the predefined template from the two institutions. All the 5,192 LDCT LCS radiology reports in the Institution-1 were collected from January 1, 2021, to December 31, 2023, for nodule-level feature retrieval and statistical analysis. The report distributions by age and sex of the three datasets are summarized in Table 2.

Dynamic Template-Constrained Decoding Method

To eliminate the formatting errors and content hallucinations of an LLM, we propose dynamic template-constrained decoding for inference. The basic idea is to use a structured and standardized template to constrain the LLM output. As shown in Figure 1, our LLM inference method takes the system instruction and the conventional report as input, uses the structured and standardized template to strictly constrain every output token during decoding, and then produces the structured report accordingly. Our approach is in sharp contrast to the existing studies, which focus on designing the system instruction to prompt LLMs [12]. However, such prompting cannot eliminate either formatting errors or content hallucinations.

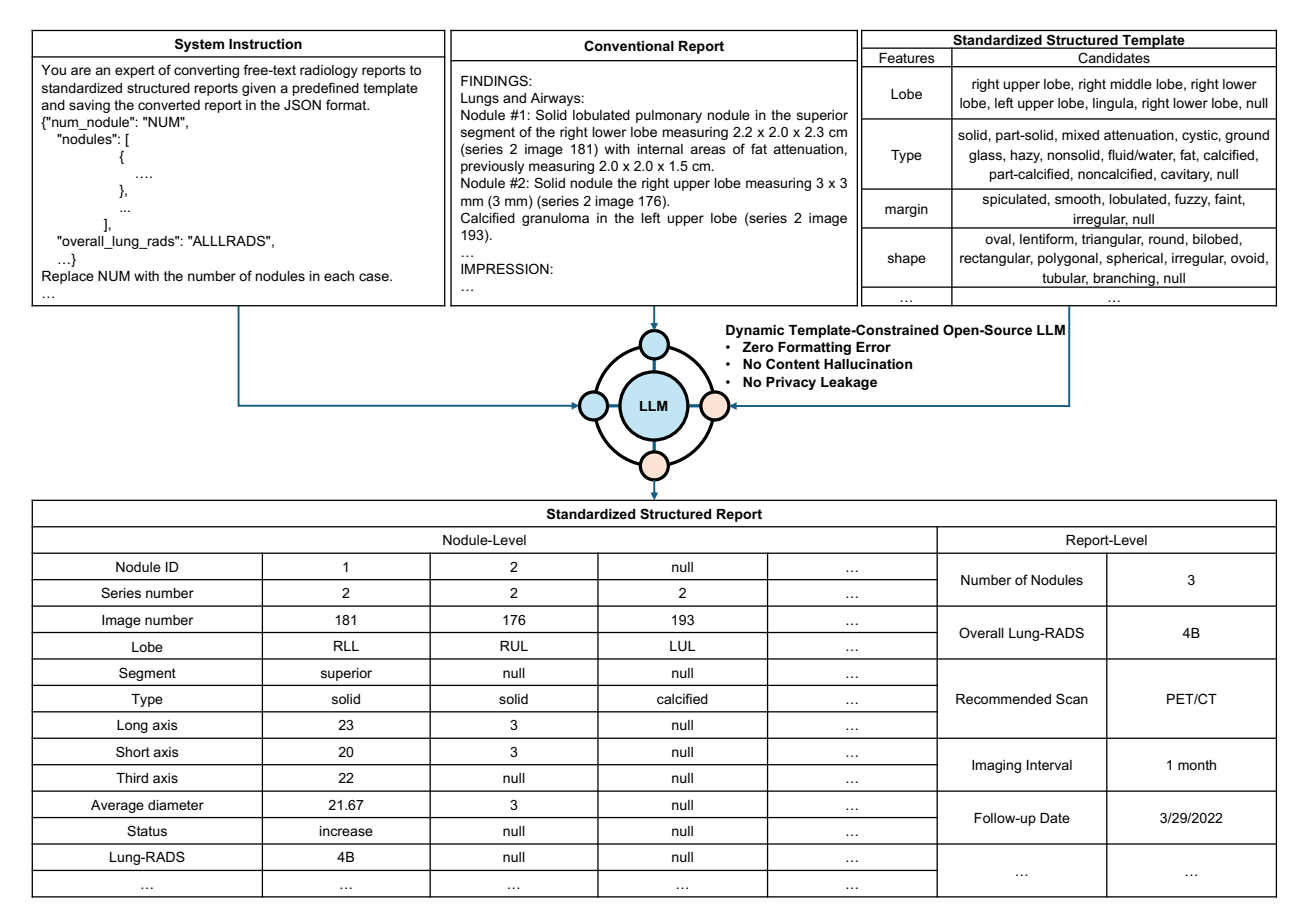


Figure 1. Framework of dynamic template-constrained LLM for level-2 structured reporting.

Specifically, we designed a dynamic template-constrained decoding method shown in Figure 2. In the common LLM inference process in Figure 2 (a), the concatenation of system instructions and free-text reports are first tokenized, the causal Transformer autoregressively calculates the probability distribution over all tokens, then a sampling strategy is implemented to sample the next token, and finally the sampled token are converted to the output text, which is also appended to the input token sequence for the next iteration. Our dynamic template-constrained inference is shown in Figure 2 (b), with the differences from the common inference highlighted in orange.

Before explaining the differences, let us introduce how to deal with the predefined template in Table 1. We represent the structured and standardized template in a dynamic JSON format with

three kinds of text: template format text without highlight, special template text highlighted in pink, and example candidate text highlighted in green, as shown in Figure 2 (c) and (d), respectively. Every special text has a candidate set defined in Table 1. To handle varying numbers of nodules reported in different reports, the dynamic template is designed to dynamically determine and create the required number of nodule descriptors (the black box of Figure 2 (c) represents a single nodule descriptor) during inference.

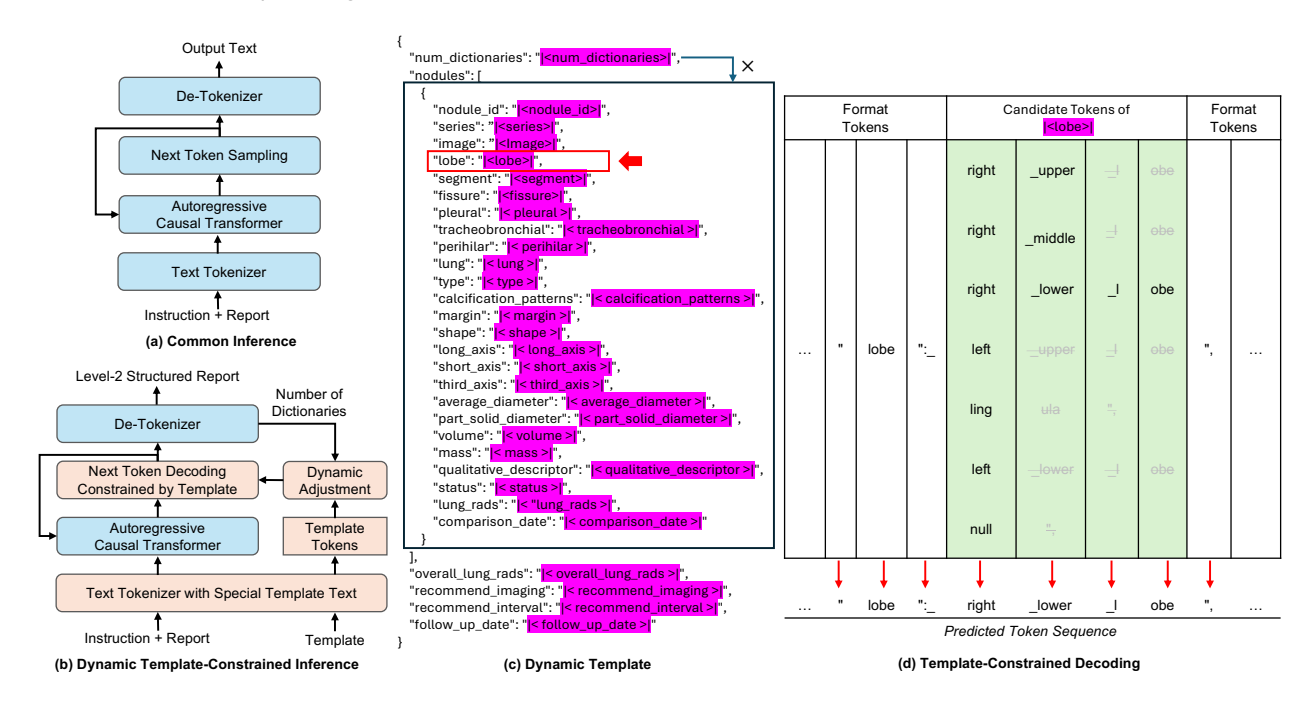


Figure 2. Dynamic template-constrained decoding. (a) The inference architecture of current LLMs, (b) our dynamic template-constrained inference architecture, (c) dynamic JSON template with added special tokens highlighted in pink, and (d) illustration of dynamic template-decoding process.

Our dynamic template-constrained decoding is detailed as follows. First, the concatenation of a system instruction, a free-text report, and a template text is tokenized. Here we added the special template text into the tokenizer so that they can be recognized and localized in the template. The template tokens include two parts: (1) the dynamic template tokens for the JSON template format text and special template text, and (2) the candidate value tokens for each special template token. During the next token prediction, we deterministically choose the token with the maximum probability over its candidate set. As shown in Figure 2 (c) and (d), the next token is autoregressively predicted along the order of dynamic template. The candidate set of the template format token only contains itself so that the output is exactly the predefined format text, ensuring no JSON formatting errors. When a special template token is recognized, its candidate token set will be used. For predicting tokens around "lobe" in Figure 2 (d), there are seven predefined candidates, and each candidate text has been tokenized into a sequence. All the seven candidate sequences are aligned from scratch. In predicting "right lower lobe", the first token is selected among "right", "left", "ling" and "null" with the maximum probability. After the "right" token is chosen, all other candidate sequences without "right" will be ignored in predicting the subsequent tokens. This process will be repeated until a compete candidate text is decoded. The number of nodule descriptors will be predicted first to adjust the template by creating the required number of nodule

descriptors. When the predicted number of nodule descriptors is zero, the "nodules" part in the JSON template will be removed.

Software Development and Open-source LLMs

Our dynamic template-constrained method was implemented based on the vLLM project [13], which is an open-source library for LLM inference and serving. In principle, our method can be applied to any LLM while its implementation needs to modify the common inference architecture. We studied its superiority on the most powerful open-source LLMs, including Llama-3.1 (8B, 70B, 405B) [10], Qwen-2 (72B) [14], and Mistral-Large (123B) [15]. All these open-sourced models were downloaded from Hugging Face with approval. We also evaluated GPT-40 on the Institution-1-labeled dataset for comparison using the same system instruction. Due to the institutional policy, the other two datasets in Table 2 are not allowed to be uploaded to any external sever to use proprietary LLMs. Since the source codes of GPT-40 is not publicly available, we cannot apply our method to it. The software development and experiments were conducted on a local server with 8x H100 GPUs. To facilitate further research of LLMs in radiology, our vLLM-Structure software, experimental scripts, example data, and tutorials have been released at https://github.com/niuchuangnn/vllm structure.

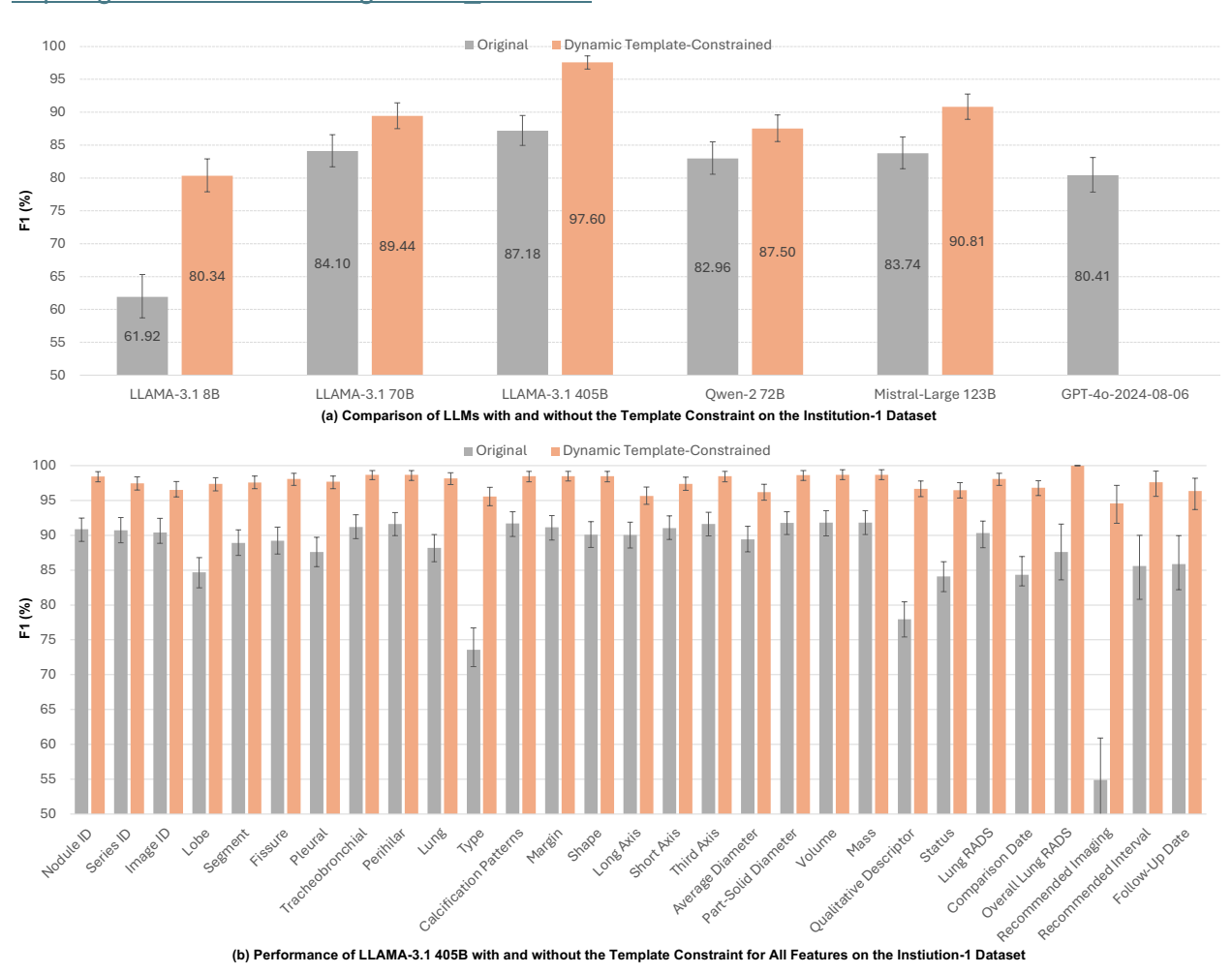


Figure 3. Comparative results of different LLMs on the Institution-1 dataset.

Automatic Structured Report Creation and Applications

All collected reports from the two institutions were automatically converted to the level-2 structured reports for pulmonary nodule descriptions using our software. All open-source LLMs were implemented in both the original inference and the proposed dynamic template-constrained decoding method. The structured reports were saved in the JSON format. All models shared the same system instruction and structured template. We further studied two use cases based on the created level-2 structured reports. Frist, a nodule-level retrieval system was built. By inputting a combination of nodule features in the retrieval system, all the individual nodules with the features will be listed and the corresponding images will be displayed. Second, the statistical distributions of various nodule features were automatically calculated by age and sex on the Insitution-1 dataset without any human annotations.

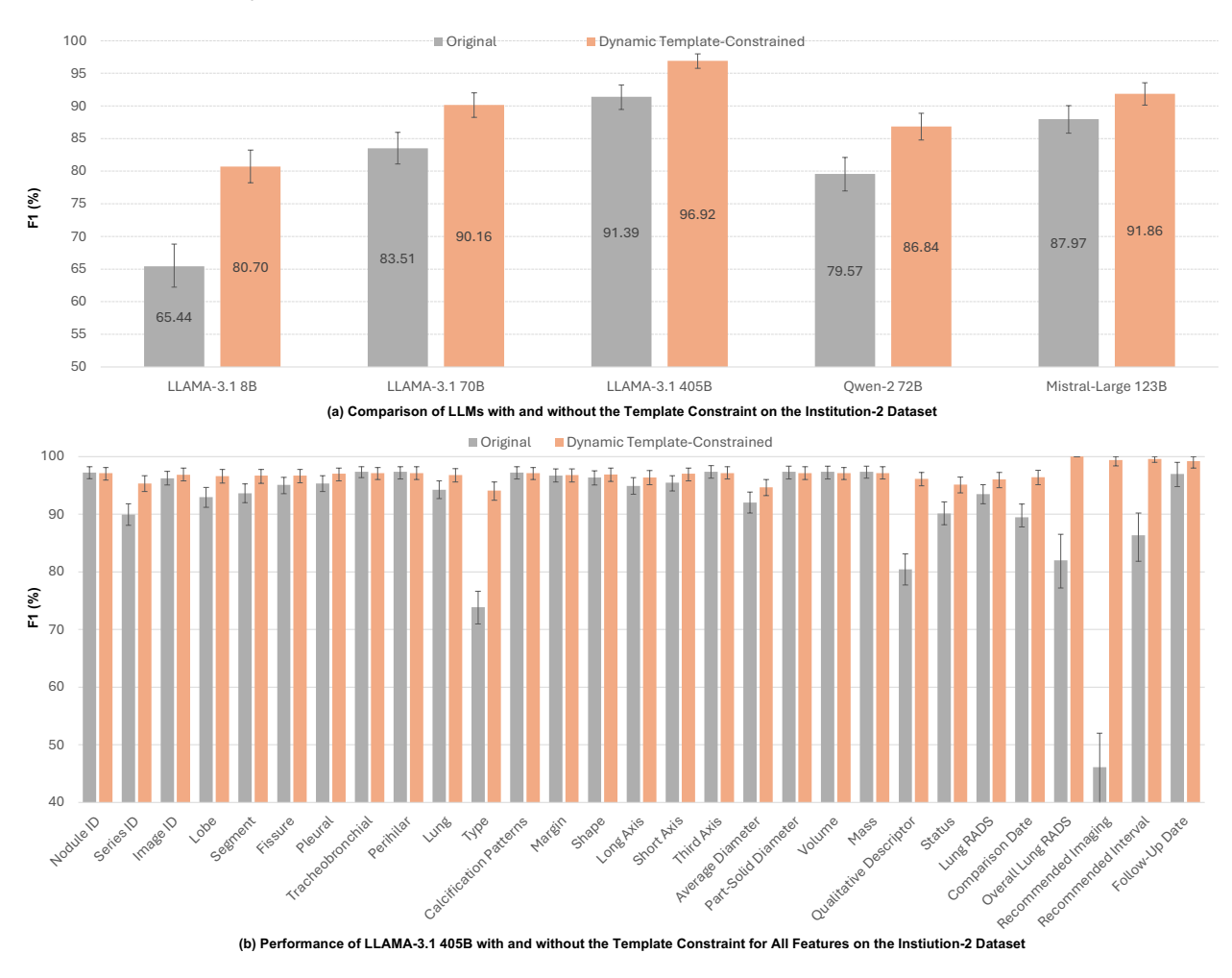


Figure 4. Comparative results of different LLMs on the Institution-2 dataset.

Data Analysis

The performance of different LLMs in creating structured reports were compared in terms of F1 score, 95% CI, and McNemar's test for each nodule feature, which measures both recall and precision. The average F1 score of all nodule features was used to measure the overall

performance, the larger the better. For nodule feature retrieval, we qualitatively presented an example. To analyze statistics, z-test was used to compare different population proportions.

RESULTS

Automatic Creation of Structured and Standardized Radiology Reports

The performance of LLMs in automatically creating the level-2 structured reports are presented in Figures 1 and Figure 2 from the free-text report on the two institutional datasets, respectively. In terms of the average performance over all lung nodule features, our method consistently improved all the open-source LLMs, including LLAMA-3.1 8B by 18.42% (F1 score: 80.34% (95% CI: 77.91%-82.88%) vs 61.92% (95% CI: 58.74%-65.34%), LLAMA-3.1 70B by 5.34% (F1 score: 89.44% (95% CI: 87.50%-91.44%) vs 84.10% (95% CI: 81.70%-86.57%), LLAMA-3.1 405B by 10.42% (F1 score: 97.60% (95% CI: 96.54%-98.55%) vs 87.18% (95% CI: 84.93%-89.49%)), Qwen-2 72B by 4.54% (F1 score: 87.50% (95% CI: 85.55%-89.61%) vs 82.96% (95% CI: 80.55%-85.50%)), Mistral-Large 123B by 7.07% (F1 score: 90.81% (95% CI: 88.94%-92.75%) vs 83.74% (95% CI: 81.39%-86.24%)), GPT-40 by 17.18% (F1 score: 97.60% (95% CI: 96.54%-98.55%) vs 80.42% (95% CI: 77.87%-83.10%)) on the institution-1 dataset; and improved LLAMA-3.1 8B by 15.26% (F1 score: 80.70% (95% CI: 78.25%-83.22%) vs 65.44% (95% CI: 62.25%-68.81%), LLAMA-3.1 70B by 6.65% (F1 score: 90.16% (95% CI: 88.27%-92.00%) vs 83.51% (95% CI: 81.11%-85.93%), LLAMA-3.1 405B by 5.53% (F1 score: 96.92% (95% CI: 95.76%-97.96%) vs 91.39% (95% CI: 89.46%-93.21%)), Qwen-2 72B by 7.27% (F1 score: 86.84% (95% CI: 84.77%-88.86%) vs 79.57% (95% CI: 76.96%-82.12%)), Mistral-Large 123B by 3.89% (F1 score: 91.86% (95% CI: 90.12%-93.54%) vs 87.97% (95% CI: 85.84%-90.03%)) on the Institution-2 dataset.

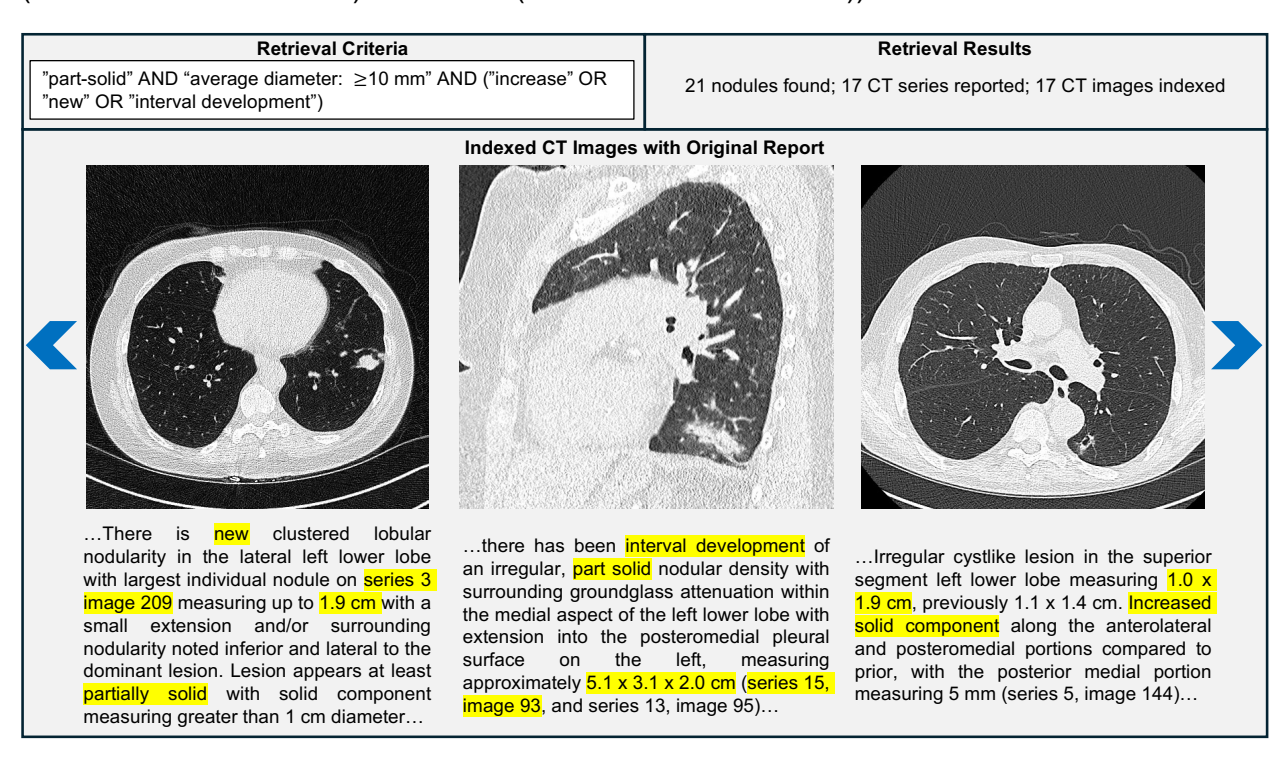


Figure 5. Use case of our nodule-level feature retrieval system based on structured radiology reports.

For the best open-source LLAMA-3.1 405B model in extracting specific nodule features, our method significantly improved the F1 scores with p-value < 0.01 for all nodule features on the Institution-1 dataset, improved the F1 scores for 21 of 29 features and had the same F1 scores for the rest 8 features, among which 18 features had p-value < 0.01, on the Institution-2 dataset. Our method also improved the F1 scores of GPT-4o for 28 of 29 nodule features with 27 features having p-value < 0.01 on the Institution-1 dataset.

Nodule-level Information Retrieval

Based on the structured reports created by the best LLM, a nodule-level feature retrieval system was prototyped and tested on the 5192 LCS reports in the Institution-1 dataset. A retrieval example is shown in Figure 5, where given the combination of retrieval features "part-solid" AND "average diameter: ≥10 mm" AND ("increase" OR "new" OR "interval development"), 21 individual nodules were retrieved, 17 of which have the series and CT image location information and displayed. The associated original reports are also shown and the relevant contents are manually highlighted.

Table 3. Distributions of Nodule Features on the Institution-1 dataset using LLM-Created Structed Reports.

		Age and Sex								
			<55 y 55-65 y			65-7		≥75 y		
Features	Total	M	F	M	F	M	F	M	F	
Total	10377 (100)	66 (0.6)	120 (1.2)	2164 (20.9)	2263 (21.8)	2317 (22.3)	2535 (24.4)	442 (4.3)	470 (4.5)	
Lobe										
	1687(16.3)	9(13.6)	22 (18.3)	360 (16.6)	361 (16.0)	379 (16.4)	404 (15.9)	68 (15.4)	84 (17.9)	
Lingula	210 (2.0)	3 (4.5)	3 (2.5)	41(1.9)	46 (2.0)	41 (1.9)	55 (2.2)	8 (1.8)	13 (2.8)	
	1385 (13.3)	12 (18.2)	18 (15.0)	303 (14.0)	267 (11.8)	315 (13.6)	358 (14.1)	57 (12.9)	55 (11.7)	
	2460 (23.7)	19 (28.8)	36 (30.0)	502 (23.2)	546 (24.1)	533 (23.0)	575 (22.7)		126 (26.8)	
RML	783 (7.5)	2 (3.0)	11 (9.2)	192 (8.9)	176 (7.8)	167 (7.2)	163 (6.4)	43 (9.7)	29 (6.2)	
	1543 (14.9)	3 (4.5)	19 (15.8)	286 (13.2)	350 (15.5)	326 (14.1)	423 (16.7)	68 (15.4)	68 (14.5)	
Lung										
Left	3523 (34.0)	27 (40.9)	43 (35.8)	748 (34.6)	737 (32.6)	811 (35.0)	857 (33.8)	141 (31.9)	159 (33.8)	
Right	5194 (50.1)	29 (43.9)	67 (55.8)	1071 (49.5)	1162 (51.3)	1131 (48.8)	1262 (49.8)	240 (54.3)	232 (49.4)	
Туре	, ,	, ,	,	, ,	` ,	, ,	, ,	, ,	, ,	
Ground Glass	696 (6.7)	4 (6.1)	13 (10.8)	97 (4.5)	186 (8.2)	105 (4.5)	200 (7.9)	23 (5.2)	68 (14.5)	
Nonsolid	090 (0.7)					` '		23 (3.2)	` ′	
Part-solid	203 (2.0)	1 (1.5)	4 (3.3)	40 (1.8)	44 (1.9)	35 (1.5)	58 (2.3)	12 (2.7)	9 (1.9)	
Solid	2027 (19.5)	28 (42.4)	20 (16.7)	439 (20.3)	491 (21.7)	400 (17.3)	492 (19.4)	94 (21.3)	63 (13.4)	
Status										
Decrease	121 (1.2)	2 (3.0)	2 (1.7)	30 (1.4)	28 (1.2)	19 (0.8)	29 (1.1)	7 (1.6)	4 (0.9)	
Increase	229 (2.2)	0 (0.0)	2 (1.7)	41 (1.9)	37 (1.6)	41 (1.8)	76 (3.0)	17 (3.8)	15 (3.2)	
Interval development	97 (0.9)	0 (0.0)	1 (0.8)	28 (1.3)	12 (0.5)	19 (0.8)	27 (1.1)	4 (0.9)	6 (1.3)	
new	851 (8.2)	12 (18.2)	10 (8.3)	154 (7.1)	183 (8.1)	200 (8.6)	200 (7.9)	37 (8.4)	55 (11.7)	
Resolved	76 (0.7)	0 (0.0)	1 (0.8)	18 (0.8)	15 (0.7)	21 (0.9)	16 (0.6)	2 (0.5)	3 (0.6)	
Average diamete	er									
<6 mm	6004 (57.9)	36 (54.5)	80 (66.7)	1279 (59.1)	1347 (59.5)	1247 (53.8)	1526 (60.2)	219 (49.5)	270 (57.4)	
6-10 mm	1226 (11.8)	8 (12.2)	11 (9.1)	236 (10.9)	219 (9.7)	314 (13.5)	317 (12.5)	80 (18.1)	41 (8.7)	
10-15 mm	246 (2.4)	4 (6.1)	4 (3.3)	32 (1.5)	37 (1.6)	75 (3.2)	56 (2.2)	18 (4.1)	20 (4.3)	
≥ 15 mm	104 (1.0)	1 (1.5)	1 (0.8)	22 (1.0)	19 (0.9)	20 (0.9)	28 (1.1)	6 (1.3)	7 (1.5)	
Overall Lung-RA										
	1162 (22.4)	10 (27.0)	21 (29.2)	290 (25.8)	283 (24.4)	272 (23.0)	227 (18.9)	30 (14.6)	29 (13.9)	
	3427 (66.0)	21 (56.8)	44 (61.1)	712 (63.5)	768 (66.1)	767 (64.7)	836 (69.7)	,	141 (67.5)	
3	238 (4.6)	0 (0.0)	2 (2.8)	48 (4.3)	48 (4.1)	57 (4.8)	53 (4.4)	12 (5.9)	18 (8.6)	
4A	167 (3.2)	1 (2.7)	1 (1.4)	37 (3.3)	30 (2.6)	41 (3.5)	43 (3.6)	5 (2.4)	9 (4.3)	
4B	85 (1.6)	0 (0.0)	1 (1.4)	16 (1.4)	10 (0.9)	20 (1.7)	19 (1.6)	12 (5.9)	7 (3.3)	
Note — M=Male	18 (0.3)	0 (0.0)	0 (0.0)	4 (0.4)	4 (0.3)	6 (0.5)	2 (0.2)	1 (0.5)	1 (0.5)	

Note.— M=Male, F=Female, LUL= left upper lobe, LLL=left lower lobe, RUL=right upper lobe, RML=right middle lobe, RLL=right lower lobe

Automatic Nodule-level Statistics

Our experiments demonstrated that nodule-level statistics can be automatically calculated from the level-2 structured reports without any need for expensive labeling of original reports. The statistics of different nodule features stratified by age and sex are summarized in Table 3. The statistical results show that the number of the extracted nodules in the upper lobes is significantly (p-value < 0.01) greater than that in other lobes, the number of the right lung is significantly (p-value < 0.01) greater than that on the left lung, female had significantly more (p-value < 0.01) ground glass nodules than male, the distribution Lung RADS scores over 0, 1, 2, 3, 4A, 4B, 4X are 1.0%, 22.4%, 66%, 4.6%, 3.2%, 1.6%, and 0.3%, respectively, where 0.8% reports did not provide lung RADS scores. The size (average diameter) distributions of lung nodules over <6 mm, 6~10 mm, 10~15 mm, ≥15 mm were 57.9%, 11.8%, 2.4%, and 1.0%, respectively, where 27% nodules did not have their sizes reported. Also, the results show that 1.2% nodules were decreased, 2.2% were increased and 0.9% were interval development, 8.2% were new nodules, and 0.7% were resolved. All the above statistical results are closely consistent with the previous findings [16-19].

DISCUSSION

Increasing evidence has shown the importance of structured radiology reporting to optimize the radiological workflow and patient outcomes. One of the major hurdles to structured reporting at level-2 is lacking an efficient and effective IT tool. Without disrupting radiologists' attention and habit, our enhanced LLM-based system can accurately and automatically create the level-2 structed reports from the free-text descriptions.

Current LLM inference cannot ensure the successful creation of the predefined structured report because of lacking a mechanism to eliminate formatting errors and content hallucinations. In contrast, our dynamic template-constrained encoding cannot only handle varying numbers of reported nodules in a dynamic template but also ensure zero formatting errors and no content hallucinations. On the other hand, most of the existing studies used proprietary LLMs, e.g., GPT-4, which requires uploading reports to the cloud server with major privacy concerns. Because of the policy and cost, these studies were conducted on relatively small datasets. Fortunately, the latest Llama 3.1 model with 405 billion parameters released on July 23, 2024, has competitive a performance with proprietary LLMs. Our developed software, vLLM-structure, can locally deploy the best open-source LLM, and enable large-scale studies without privacy concerns. Importantly, our method significantly and consistently improved existing models on cross-institutional datasets. The best accuracy of our enhanced LLM achieved ~97% F1 score on both institution datasets. Considering that dynamic templating for lung nodule reporting is complex, achieving such a high accuracy has strongly demonstrated the feasibility of using our LLM-based tool for structured radiology reporting at level-2.

Thanks to the standardized and quantified items in structured reporting, large-scale data mining becomes easy. We have shown two use cases of structured radiology reports in nodule-level feature retrieval and automatic statistical analysis. The inputs can be any combination of nodule features, then all individual nodules and the associated images will be retrieved. Additionally, more electronic medical records could be linked with the structured radiology reports to build more

advanced systems. Our nodule-level retrieval system may be used for diagnosis, therapy, research, teaching, and other purposes. Furthermore, we have conducted an automatic statistical analysis on a large-scale LCS report dataset. The high evaluation accuracy and the consistent statistical results to prior findings suggest the effectiveness and reliability of LLM-based statistics. Promisingly, large-scale multi-institutional statistics on historical data become straightforward though LLM-based structured reporting. Moreover, quantitative data of the structured reports can be directly used for training and validating AI models on large-scale datasets [20, 21].

There were limitations to this study. We only conducted retrospective experiments and created level-2 structured reports from existing reports. The prospective studies could be conducted by deploying our software in the reporting workflow to study the effectiveness of creating structured reports through interactions between LLMs and radiologists. We built the standardized template and created the structured reports only for lung nodule reproting without including other potential abnormalities. However, lung nodule reporting is the core component in LCS, which is representative and extendable. Although we built a standardized template for lung nodules in this cross-institutional study, it is neither formally adopted nor immediately ready to use in practice. Nevertheless, this study is informative and encouraging to demonstrate our LLM-based solution to structed radiology reporting.

In conclusion, we have proposed a dynamic template-constrained LLM to create structured reports at level-2 from the free-text descriptions. Our method has achieved the state-of-the-art accuracy without formatting errors, content hallucinations, or privacy concerns. We have demonstrated the workflow from building the standardized template to creating structured reports with our developed software for LCS. The accuracy and superiority of LLMs with our inference method have been evaluated on cross-institutional datasets. We have successfully demonstrated the utilities and merits of structured reporting in nodule-level retrieval and automatic statistical analysis on a large-scale dataset. Our open-source software, vLLM-structure, is publicly available for further translational research on structured radiology reporting.

References

- [1] J. M. Nobel, K. van Geel, and S. G. F. Robben, "Structured reporting in radiology: a systematic review to explore its potential," *European Radiology,* vol. 32, no. 4, pp. 2837-2854, 2022/04/01, 2022.
- [2] D. B. Larson, A. J. Towbin, R. M. Pryor, and L. F. Donnelly, "Improving consistency in radiology reporting through the use of department-wide standardized structured reporting," *Radiology*, vol. 267, no. 1, pp. 240-250, 2013.
- J. M. Nobel, E. M. Kok, and S. G. F. Robben, "Redefining the structure of structured reporting in radiology," *Insights into Imaging*, vol. 11, no. 1, pp. 10, 2020/02/04, 2020.
- [4] R. European Society of, "ESR paper on structured reporting in radiology," *Insights into Imaging*, vol. 9, no. 1, pp. 1-7, 2018/02/01, 2018.
- [5] D. P. dos Santos, E. Kotter, P. Mildenberger, L. Martí-Bonmatí, and R. European Society of, "ESR paper on structured reporting in radiology—update 2023," *Insights into Imaging*, vol. 14, no. 1, pp. 199, 2023/11/23, 2023.
- [6] D. Harris, D. M. Yousem, E. A. Krupinski, and M. Motaghi, "Eye-tracking differences between free text and template radiology reports: a pilot study," *Journal of Medical Imaging*, vol. 10, no. S1, pp. S11902-S11902, 2023.
- [7] L. C. Adams, D. Truhn, F. Busch, A. Kader, S. M. Niehues, M. R. Makowski, and K. K. Bressem, "Leveraging GPT-4 for Post Hoc Transformation of Free-text Radiology Reports into Structured Reporting: A Multilingual Feasibility Study," *Radiology*, vol. 307, no. 4, pp. e230725, 2023.
- [8] R. Bhayana, B. Nanda, T. Dehkharghanian, Y. Deng, N. Bhambra, G. Elias, D. Datta, A. Kambadakone, C. G. Shwaartz, C.-A. Moulton, D. Henault, S. Gallinger, S. Krishna, and K. Fowler, "Large Language Models for Automated Synoptic Reports and Resectability Categorization in Pancreatic Cancer," *Radiology*, vol. 311, no. 3, pp. e233117, 2024.
- [9] L. C. Adams, D. Truhn, F. Busch, F. Dorfner, J. Nawabi, M. R. Makowski, K. K. Bressem, and L. Moy, "Llama 3 Challenges Proprietary State-of-the-Art Large Language Models in Radiology Board–style Examination Questions," *Radiology*, vol. 312, no. 2, pp. e241191, 2024.
- [10] A. Dubey, A. Jauhri, A. Pandey, A. Kadian, A. Al-Dahle, A. Letman, A. Mathur, A. Schelten, A. Yang, and A. Fan, "The llama 3 herd of models," *arXiv preprint arXiv:2407.21783*, 2024.
- [11] T. Nakaura, R. Ito, D. Ueda, T. Nozaki, Y. Fushimi, Y. Matsui, M. Yanagawa, A. Yamada, T. Tsuboyama, N. Fujima, F. Tatsugami, K. Hirata, S. Fujita, K. Kamagata, T. Fujioka, M. Kawamura, and S. Naganawa, "The impact of large language models on radiology: a guide for radiologists on the latest innovations in AI," *Japanese Journal of Radiology,* vol. 42, no. 7, pp. 685-696, 2024/07/01, 2024.
- [12] Q. Lyu, J. Tan, M. E. Zapadka, J. Ponnatapura, C. Niu, K. J. Myers, G. Wang, and C. T. Whitlow, "Translating radiology reports into plain language using ChatGPT and GPT-4 with prompt learning: results, limitations, and potential," *Visual Computing for Industry, Biomedicine, and Art*, vol. 6, no. 1, pp. 9, 2023/05/18, 2023.
- [13] W. Kwon, Z. Li, S. Zhuang, Y. Sheng, L. Zheng, C. H. Yu, J. Gonzalez, H. Zhang, and I. Stoica, "Efficient memory management for large language model serving with pagedattention." pp. 611-626.
- [14] A. Yang, B. Yang, B. Hui, B. Zheng, B. Yu, C. Zhou, C. Li, C. Li, D. Liu, and F. Huang, "Qwen2 technical report," arXiv preprint arXiv:2407.10671, 2024.
- [15] Mistral. "https://huggingface.co/mistralai/Mistral-Large-Instruct-2407," Sep 23, 2024.
- [16] J. E. Walter, M. A. Heuvelmans, and M. Oudkerk, "Small pulmonary nodules in baseline and incidence screening rounds of low-dose CT lung cancer screening," *Translational Lung Cancer Research*, vol. 6, no. 1, pp. 42-51, 2017.

- [17] A. R. Larici, A. Farchione, P. Franchi, M. Ciliberto, G. Cicchetti, L. Calandriello, A. Del Ciello, and L. Bonomo, "Lung nodules: size still matters," *European respiratory review,* vol. 26, no. 146, 2017.
- [18] J. Christensen, A. E. Prosper, C. C. Wu, J. Chung, E. Lee, B. Elicker, A. R. Hunsaker, M. Petranovic, K. L. Sandler, B. Stiles, P. Mazzone, D. Yankelevitz, D. Aberle, C. Chiles, and E. Kazerooni, "ACR Lung-RADS v2022: Assessment Categories and Management Recommendations," *Journal of the American College of Radiology,* vol. 21, no. 3, pp. 473-488, 2024.
- [19] J. Cai, M. Vonder, G. J. Pelgrim, M. Rook, G. Kramer, H. J. M. Groen, G. H. de Bock, R. Vliegenthart, and A. de Roos, "Distribution of Solid Lung Nodules Presence and Size by Age and Sex in a Northern European Nonsmoking Population," *Radiology*, vol. 312, no. 2, pp. e231436, 2024.
- [20] C. Niu, Q. Lyu, C. D. Carothers, P. Kaviani, J. Tan, P. Yan, M. K. Kalra, C. T. Whitlow, and G. Wang, "Specialty-Oriented Generalist Medical AI for Chest CT Screening," arXiv:2304.02649, 2024.
- [21] C. Niu, and G. Wang, "Unsupervised contrastive learning based transformer for lung nodule detection," *Physics in Medicine & Biology*, vol. 67, no. 20, pp. 204001, 2022.